The Impact of High Order Refraction on Optical Microbubble Sizing in Multiphase Flows

by

H.-H. Qiu[(1)] and C. T. Hsu[(2)]

Department of Mechanical Engineering
Hong Kong University of Science and Technology, Clear Water Bay, Kowloon
Hong Kong, SAR China
[(1)]E-mail: meqiu@ust.hk
[(2)]E-mail: mecthsu@ust.hk

Abstract

The measurements of bubble size and velocity in multiphase flows are important in many researches and industrial applications. It has been found that the high order refraction has great impact on PDA sizing method when the relative refractive index of media is less than one. Although the spatial frequencies of first order refraction and surface reflection become identical at the optimized scattering angle by using previously proposed method, the second order, as well as high order, refractions can not be neglected, because of different spatial frequency and motion direction. The problem has been investigated and a model of phase-size correlation, which also takes the high order refractions into consideration, is introduced to improve the accuracy of bubble sizing. In this study a method based on the recently developed dual mechanisms' scattering model was further developed. Two scattering phases measured by photodetectors are used to calculate the particle size. By utilizing the conversion factor of second order refraction, as well as some high order refractions, the particle diameter can be solved numerically. Hence, the model relaxes the assumption of single scattering mechanism in conventional phase-Doppler anemometry. To demonstrate the capability of the newly developed method, the model was simulated numerically by using Generalized Lorenz Mie Theory (GLMT). The optical parameters such as the measurement volume size, the focus lengths of the sending and receiving lenses, the size and shape of the receiving aperture, the particle size and its trajectory, and the phase conversion factors are used to analyze the performance of the newly developed method. The results of simulation are compared with those based on the conventional method. An optimization method for accurately sizing air-bubble in water has been suggested.

1. Introduction

Phase-Doppler Anemometry (PDA) is nowadays widely used for velocity measurement and particle sizing in experimental studies of multiphase flows. Various developments were made to extend the application area of PDA. The accurate measurement of droplet size is the utmost important since the bubble volume depends on the third power of the bubble diameter. To achieve high spatial resolution, it is often required to decrease the measurement volume size. Unfortunately, a simple reduction in the measurement volume size can cause the phenomena in conflict with the assumption of a uniform illumination. Consequently, the result suffers from error in sizing large particles due to the nonlinearity in the phase/diameter relationship because the beam intensity is practically nonuniform [1-9]. Various solutions to minimize the trajectory ambiguity have been proposed for classical geometry [5-9]. However, all of above methods for the elimination of the measurement volume effect (MVE) are based on a signal validation scheme, which may cause the complexity in the determination of measurement volume size. The consequence is that the calibration method could be very complicated.

The recent study [10] developed a new approach by taking both the refraction and reflection into account. The validation experiments based on this method demonstrated successfully in measuring particles with refractive index greater than one [11]. The Gaussian beam defect and slit effect can be eliminated according to the validation experiments [11]. However, the previous simulations and experiments were only conducted for the case of refractive index greater than one. It was found that the second order internal refraction could have great impact on the particle sizing if the relative refractive index is less than one (e.g. in bubbly flows) [12]. In this study a method based on the recently developed dual mechanisms' scattering model [10, 11] was further developed. In this method two scattering phases measured by photodetectors are used to calculate the particle size. It is found that although the spatial frequencies of first order refraction and surface reflection become identical at the optimized scattering angle as suggested by [10], the second order refraction can not be neglected, because of different spatial frequency and motion direction. By utilizing the conversion factor of the second order refraction, the particle diameter can be solved numerically. To demonstrate the capability of the newly developed method, the model was simulated numerically by using Generalized Lorenz Mie Theory (GLMT) [5]. The optical parameters, such as the measurement volume size, the focus lengths of the sending and receiving lenses, the size and shape of the receiving aperture, the particle size and its trajectory, and the phase conversion factors, are used to analyze the performance of the newly developed method.

2. Analytical Description

Figure 1 shows a recently improved 4-detector PDA system, where the receiving optics consists of four detectors that are symmetrically orientated with elevation angles ψ_1 and ψ_2 for outer and inner detector pairs, respectively.

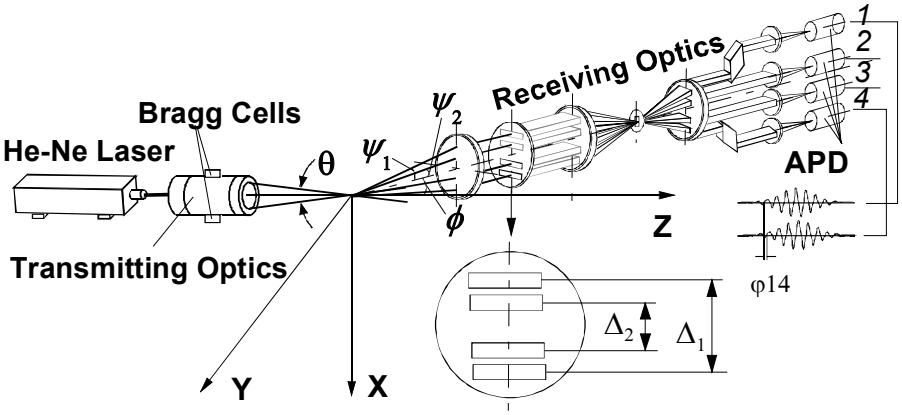

Figure 1 Optical layout of four-detector phase Doppler anemometry: APD, avalanche photodiode

The phase differences $\varphi 14$ and $\varphi 23$ between the two outer and inner detectors can be determined from the two Doppler signal pairs. The light scattering patterns from a bubble in the measurement volume of the PDA system are shown in Fig. 2.

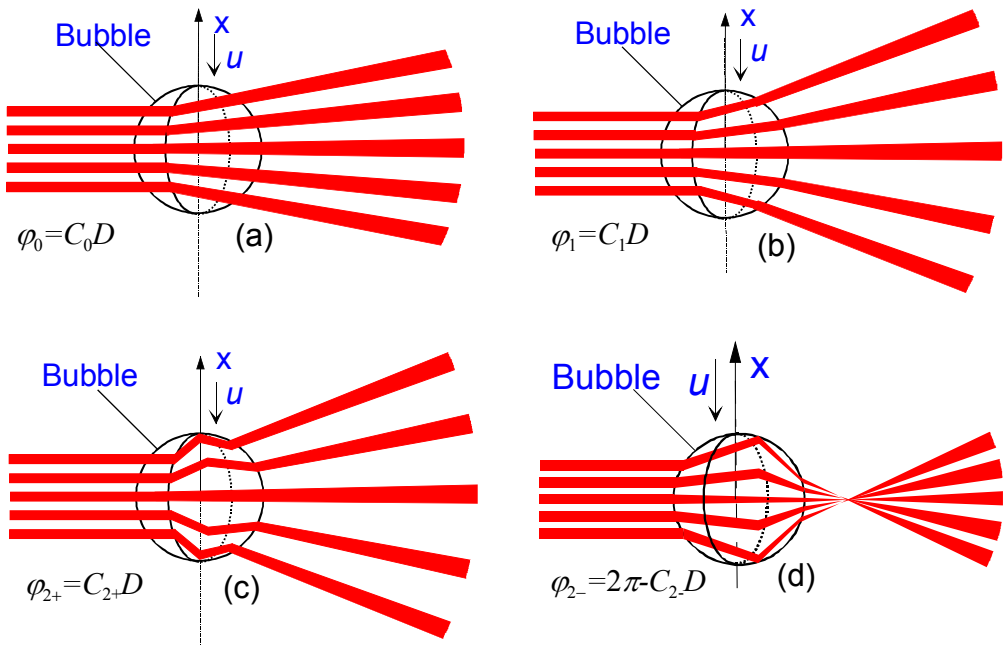

Figure 2 Bubble scattering fringe patterns

According to the bubble geometric scattering rays shown in Figs. 3 and 4, and the coordinates shown in Fig. 5. we have

$$n_m \sin\beta_p = n_b \sin\beta_p' \quad ; \quad m = n_b/n_m \tag{1}$$

$$\sin\beta_p = \frac{y_p}{r} \tag{2}$$

$$\tan\alpha = \frac{\delta f}{2y_p} \approx \sin\alpha \tag{3}$$

where β_p denotes the incident angle for each scattering mechanism, $\delta f = \frac{\lambda}{2n_m \sin(\theta/2)}$ is the incident fringe spacing in the measurement volume, and p = 0, 1, 2, …, denote the surface reflection, first order refraction, second order refraction and so on for both positive and negative sides respectively.

The relation of scattering angle ϕ_p and incident angle β can be described as

$$\phi_p = \pi(1-p) - 2\beta_p + 2p\arcsin\left(\frac{1}{m}\sin\beta_p\right) \quad \text{for } y > 0 \tag{4}$$

and

$$\phi_p = \pi(p-1) + 2\beta_p - 2p\arcsin\left(\frac{1}{m}\sin\beta_p\right) \quad \text{for } y < 0 \tag{5}$$

where the scattering angle ϕ is also called the off-axis angle of the receiving unit and β_p is determined on the bubble surface. It is important to note that the off-axis angle (the scattering angle in above equations) is always assumed to be positive because all the scattering rays are received by the receiving unit. The phase-size conversion factors of different scattering mechanisms can be described as

$$C_{p\pm} = \frac{720\tan(\psi)\sin(\beta_{p\pm})\sin\left(\frac{\theta}{2}\right)}{\lambda\sin(\phi)} \tag{6}$$

where θ, ϕ and ψ are as defined in Figure 1. The subscripts "+" and "-" are used for describing y>0 and y<0, respectively. It is clear that the measured phase is contributed by both reflection and refractions, which coexist in most cases. Therefore, the problem is not one of being dominated by either reflection or refractions but a combination of all of them.

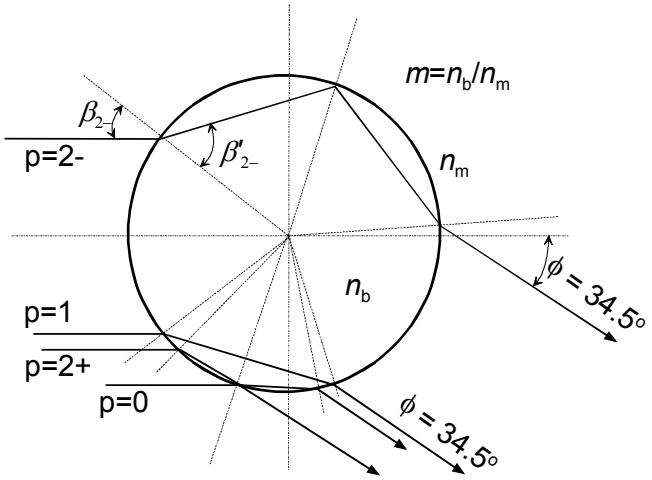

Figure 3 Description of different scattering mechanisms at an arbitrary scattering angle (m=1/1.33)

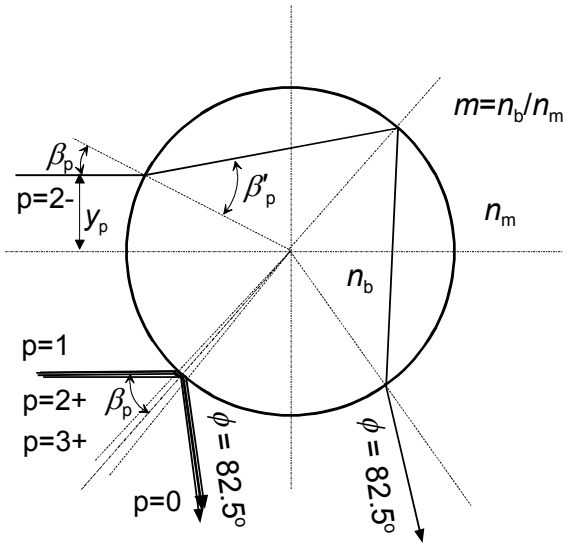

Figure 4 Description of different scattering mechanisms at the optimized orientation angle (m=1.33)

By using previous research results, the surface reflection (p=0) and first order refraction (p=1) for the incident rays from y > 0 side can be easily obtained as below

$$\beta_{0+} = \frac{\pi}{2} - \frac{\phi}{2} \tag{7}$$

$$\beta_{1+} = \frac{\pi}{2} - \arccos\left(\sqrt{\frac{m^2 \sin^2\left(\frac{\phi}{2}\right)}{1+m^2-2m\cos\left(\frac{\phi}{2}\right)}}\right) \tag{8}$$

where m and ϕ are the relative refractive index and the off-axis angle, respectively. It is clear that the surface reflection and first order refraction from $y<0$ side are unable to reach $\phi>0$ side as shown in Figure 3 and Figure 4.

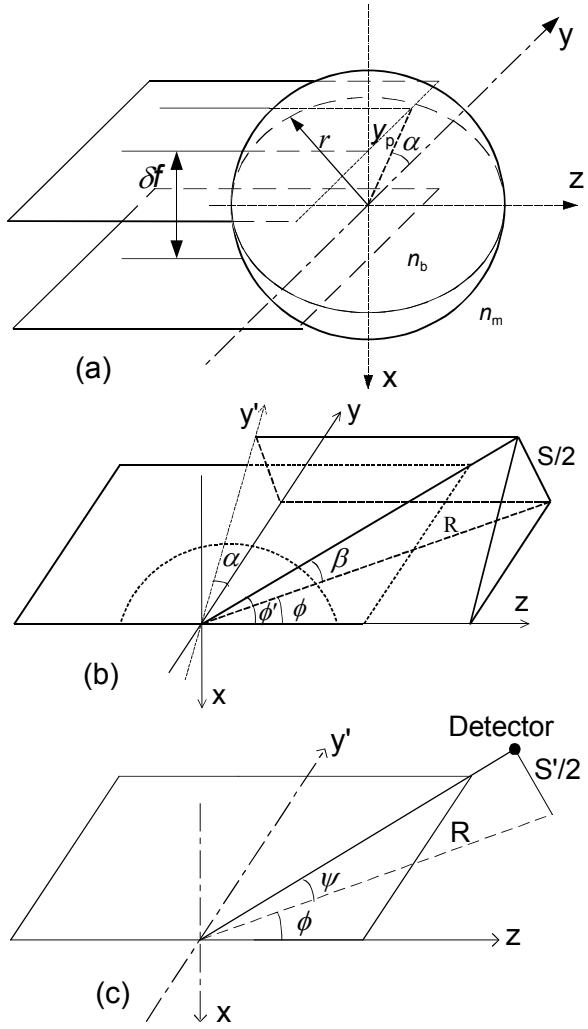

Figure 5 Geometry of Single Bubble Scattering

For second order refractions, substituting p=2 into equations (4) and (5) and assuming $\tau_2 = \frac{\pi}{2} - \beta_2$, we have:

$$\cos\tau_2 = m\cos\left(\frac{2\tau_2+\phi_2}{4}\right) \qquad \text{for } y > 0 \tag{9}$$

$$\cos\tau_2 = m\cos\left(\frac{2\tau_2-\phi_2}{4}\right) \qquad \text{for } y < 0 \tag{10}$$

i.e.

$$\cos\tau_2 = m\cos\left(\frac{2\tau_2 \pm \phi_2}{4}\right) \tag{11}$$

Equation (11) can be re-written as

$$2\cos^2\frac{\tau_2}{2} - 1 - m\cos\frac{\phi}{4}\cos\frac{\tau_2}{2} = \pm m\sin\frac{\phi}{4}\sqrt{1-\cos^2\frac{\tau_2}{2}} \tag{12}$$

Let $x = \cos\frac{\tau_2}{2}$, the following forth order polynomial equation can be obtained:

$$x^4 - m\cos\frac{\phi}{4}x^3 + \frac{m^2-4}{4}x^2 + \frac{m\cos\frac{\phi}{4}}{2}x + \frac{1-m^2\sin^2\frac{\phi}{4}}{4} = 0 \tag{13}$$

Solving equation (13), as a result, the incident angles of second order refraction for both positive and negative sides are

$$\beta_{2+} = \frac{\pi}{2} - 2\arccos(x_{2+}) \tag{14}$$

$$\beta_{2-} = \frac{\pi}{2} - 2\arccos(x_{2-}) \tag{15}$$

where x_{+}, x_{-}, a, b, c, and d are described in the following Eqs. (16)-(20).

$$x_{2+} = \frac{1}{2}\left(-\frac{\left(a-\sqrt{8y_1+a^2-4b}\right)}{2} + \sqrt{\frac{\left(a-\sqrt{8y_1+a^2-4b}\right)^2}{4} - 4\left(y_1 - \frac{(ay_1-c)}{\sqrt{8y_1+a^2-4b}}\right)}\right) \tag{16}$$

$$x_{2-} = \frac{1}{2}\left(-\frac{\left(a-\sqrt{8y_1+a^2-4b}\right)}{2} - \sqrt{\frac{\left(a-\sqrt{8y_1+a^2-4b}\right)^2}{4} - 4\left(y_1 - \frac{(ay_1-c)}{\sqrt{8y_1+a^2-4b}}\right)}\right) \tag{17}$$

$$a = -m\cos\left(\frac{\phi}{4}\right),\quad b = \frac{m^2-4}{4},\quad c = \frac{1}{2}m\cos\left(\frac{\phi}{4}\right),\quad d = \frac{1-m^2\sin^2\left(\frac{\phi}{4}\right)}{4}; \tag{18}$$

$$p = \frac{3(a\cdot c - 4d) - b^2}{12}, \qquad q = \frac{-2b^3 + 9b\cdot(a\cdot c - 4d) + 27\left(d\left(4b-a^2\right) - c^2\right)}{216} \tag{19}$$

$$\Delta = \frac{q^2}{4} + \frac{p^3}{27}, \qquad y_1 = \left(-\frac{q}{2} + \sqrt{\Delta}\right)^{\frac{1}{3}} + \left(-\frac{q}{2} - \sqrt{\Delta}\right)^{\frac{1}{3}} + \frac{b}{6} \tag{20}$$

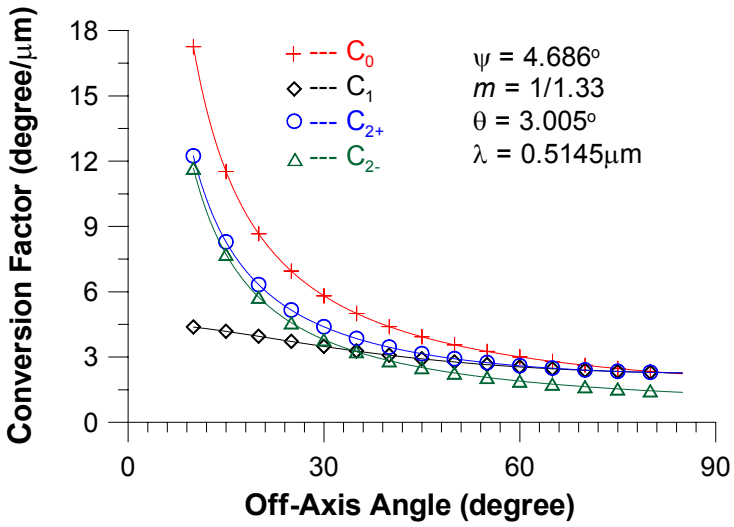

Figure 6 Phase-Size Conversion Factors for Different Scattering Mechanisms

The calculated phase-size conversion factors C_0, C_1, C_{2+}, and C_{2-} are shown in Figure 6. As indicated by previous researches, for a particle passing through the focused beams along different trajectories, the balance between the reflected and refracted rays will vary. This trajectory dependence can lead to significant errors. In Figure 6, it is found that $C_0 = C_1$ at ϕ=82.5 which is called the optimized angle, as described by Qiu and Hsu [10]. It is important to know that C_{2+}, C_0, and C_1 are also identical at this optimized angle for m=1/1.33. Furthermore, from Figure 2 we also know that the fringe patterns of reflection, first, second and higher order refractions in y>0 side move in the same direction.

Therefore, it is anticipated that for all higher order refractions from y > 0 side the contributions to the phase-size conversion factors have identical effect on the particle sizing if an optimized off-axis angle (scattering angle) is selected. To prove this assumption, determine the optimized off-axis angle (scattering angle) using the following Eq. (21) [10]:

$$\phi_p = \arccos\left(2m^2 - 1\right) = \pi - 2\arcsin(m) \tag{21}$$

Substituting Eq. (21) into Eq. (4), we have

$$\phi_p = \pi - 2\arcsin(m) = \pi(1-p) - 2\beta_p + 2p\arcsin\left(\frac{1}{m}\sin\beta_p\right) \tag{22}$$

Hence,

$$\frac{1}{m}\sin\beta_p = \cos\left[\frac{1}{p}\left(\arcsin(m) - \beta_p\right)\right] \tag{23}$$

The solution is

$$\beta_p = \arcsin(m) \tag{24}$$

Equation (24) shows if the optimized off-axis angle based on Eq. (4) is selected the incident angles β_p , (p=0,1,2, …) are identical each other, i.e., all phase-size conversion factors calculated by Eq. (6) are also identical. Therefore, for y>0 side the contributions of all higher order scattering rays become identical at this optimized off-axis angle and we can use an overall intensity and phase-size conversion factor C_0 to represent it. As a result, we only need to consider the effect of higher order refractions from y<0 side. In this only the second order refraction from y<0 side will be considered because it plays the most important role in the bubble sizing. Since the negative side second order refraction moves towards the opposite direction of the particle motion (see Fig. 2), a combined scattering model can be obtained by providing that the phase-size relations for a four detector system [10].

The relationship between the measured phases from multi-detectors and optical parameters can be described in Eqs. (25) and (26), where $C1_p$ and $C2_p$ are the phase-size conversion factors for phases φ14 and φ23, respectively.

$$\varphi_{14} = 2\arctan\left[\frac{I1_{2-}\sin\left(\frac{C1_{2-}D}{2}\right) - I1_0\sin\left(\frac{C1_0D}{2}\right)}{I1_{2-}\cos\left(\frac{C1_{2-}D}{2}\right) + I1_0\cos\left(\frac{C1_0D}{2}\right)}\right] \tag{25}$$

$$\varphi_{23} = 2\arctan\left[\frac{I2_{2-}\sin\left(\frac{C2_{2-}D}{2}\right) - I2_0\sin\left(\frac{C2_0D}{2}\right)}{I2_{2-}\cos\left(\frac{C2_{2-}D}{2}\right) + I2_0\cos\left(\frac{C2_0D}{2}\right)}\right] \tag{26}$$

where $I1_0$ and $I2_0$, are the overall intensities from y>0 side's scattering rays for outer and inner receivers. $I1_{2-}$ and $I2_{2-}$ are the intensities from y<0 side's scattering rays for outer and inner receivers, respectively.

In a practical PDA system the elevation angle of each detector pair is quite small and the sensitivities of each avalanche photodiode are adjusted normally to achieve uniform amplitude in the output signals. Hence the scattering intensities can be assumed the same for each detector. In this case $I1_0 \approx I2_0 = I_0$ and $I1_{2-} \approx I2_{2-} = I_{2-}$ can be assumed which has also been proved by GLMT simulations.

Therefore,

$$\varphi_{14} = 2\arctan\left[\frac{I_{2-}\sin\left(\frac{C1_{2-}D}{2}\right) - I_0\sin\left(\frac{C1_0D}{2}\right)}{I_{2-}\cos\left(\frac{C1_{2-}D}{2}\right) + I_0\cos\left(\frac{C1_0D}{2}\right)}\right] \tag{27}$$

$$= 2\arctan\left[\frac{\frac{I_{2-}}{I_{2-}+I_0}\sin\left(\frac{C1_{2-}D}{2}\right) - \left(1-\frac{I_{2-}}{I_{2-}+I_0}\right)\sin\left(\frac{C1_0D}{2}\right)}{\frac{I_{2-}}{I_{2-}+I_0}\cos\left(\frac{C1_{2-}D}{2}\right) + \left(1-\frac{I_{2-}}{I_{2-}+I_0}\right)\cos\left(\frac{C1_0D}{2}\right)}\right]$$

$$\varphi_{23} = 2\arctan\left[\frac{I_{2-}\sin\left(\frac{C2_{2-}D}{2}\right) - I_0\sin\left(\frac{C2_0D}{2}\right)}{I_{2-}\cos\left(\frac{C2_{2-}D}{2}\right) + I_0\cos\left(\frac{C2_0D}{2}\right)}\right] \tag{28}$$

$$= 2\arctan\left[\frac{\frac{I_{2-}}{I_{2-}+I_0}\sin\left(\frac{C2_{2-}D}{2}\right) - \left(1-\frac{I_{2-}}{I_{2-}+I_0}\right)\sin\left(\frac{C2_0D}{2}\right)}{\frac{I_{2-}}{I_{2-}+I_0}\cos\left(\frac{C2_{2-}D}{2}\right) + \left(1-\frac{I_{2-}}{I_{2-}+I_0}\right)\cos\left(\frac{C2_0D}{2}\right)}\right]$$

can be obtained. Combining Eqs. (27) and (28), and eliminating $\frac{I_0}{I_{2-}+I_0}$ term, the following solution can be obtained:

$$\frac{\left(-\cos\left(\frac{C1_{2-}D}{2}\right)\tan\left(\frac{\varphi 14}{2}\right) - \sin\left(\frac{C1_{2-}D}{2}\right)\right)}{\left(\tan\left(\frac{\varphi 14}{2}\right)\left(\cos\left(\frac{C1_0D}{2}\right) - \cos\left(\frac{C1_{2-}D}{2}\right)\right) - \sin\left(\frac{C1_0D}{2}\right) - \sin\left(\frac{C1_{2-}D}{2}\right)\right)} -$$
$$\frac{\left(-\cos\left(\frac{C2_{2-}D}{2}\right)\tan\left(\frac{\varphi 23}{2}\right) - \sin\left(\frac{C2_{2-}D}{2}\right)\right)}{\left(\tan\left(\frac{\varphi 23}{2}\right)\left(\cos\left(\frac{C2_0D}{2}\right) - \cos\left(\frac{C2_{2-}D}{2}\right)\right) - \sin\left(\frac{C2_0D}{2}\right) - \sin\left(\frac{C2_{2-}D}{2}\right)\right)} = 0 \tag{29}$$

Note that the conversion factor C_{2-} does not equal to the C_0 at the optimized off-axis angle. In Eq. (29) the only unknown is the bubble diameter, D, and therefore, it can be determined if $\varphi 14$ and $\varphi 23$ can be measured.

3. Results and Discussion

To evaluate the performance of the new method, Generalized Lorenz Mie Theory (GLMT) was used to simulate MVE in comparison with that based on the conventional single scattering mechanism assumption. Simulations of the MVE were carried out for the system geometry as shown in Figure 1 with the parameters given in Table 1. The equation used in [10] was adopted to determine the optimized off-axis angle. For the conventional method, only the inner detector pair is used in the simulation. The major direction of particle motion was in the Y direction, which is most critical in practical cases. The result of simulations is shown in Figs. 7-10.

Table 1 Optical parameters

Parameters	Value	Unit
Wavelength (λ)	0.5145	μm
Radius of Beam Waist (r_0)	40	μm
Transmitting Angle θ	3.06	degree
Receiving Elevation Angle ψ_1	4.686	degree
Receiving Elevation Angle ψ_2	2.343	degree
Off-Axis Angle φ	82.5	degree
Relative Refractive Index m	0.7518	

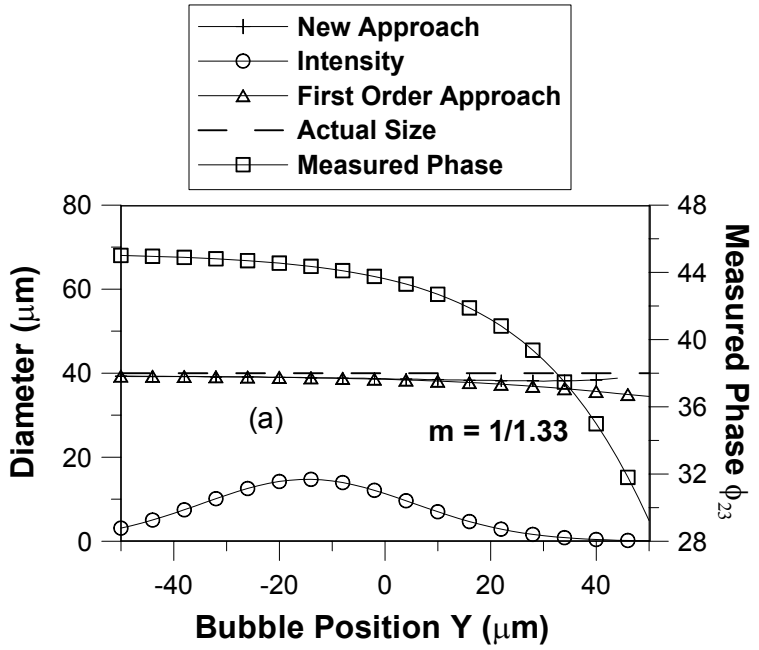

Figure 7 Phase-measurement results among the conventional, the first order and the new approaches

As shown in Fig. 7, the measured diameters for both the conventional, first order approach and the newly developed methods are almost identical with an ideal diameter 40 μm. This is because for a given droplet diameter smaller than the measurement-volume diameter, the second order MVE can normally be neglected. If the droplet diameter is larger than the diameter of the measurement volume, the MVE becomes significant as shown in Figs. 7-10.

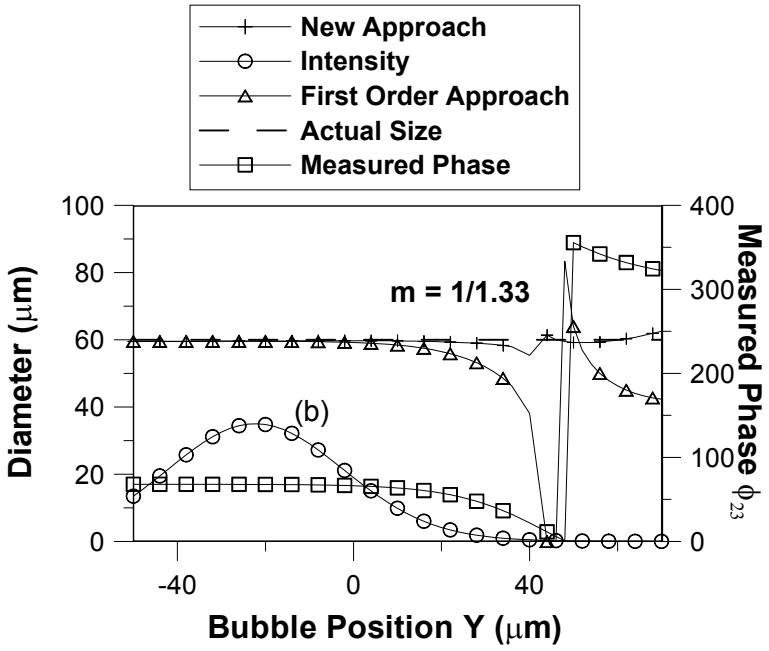

Figure 8 Phase-measurement results among the conventional, the first order and the new approaches

As shown in Fig. 8, a 60 μm air bubble passing through the measurement volume parallel to the *Y* axis at z = 0 μm will yield a large-phase transition (> 100% in this special case) owing to the change of the scattering mechanisms from reflection to refraction. If the phase is determined by the conventional and first order approach methods, a large measurement error may occur. Only a very small fluctuation (< 3%) in the phase

determination from using Eq. (29), hence the MVE, can be neglected. Figs. 9 and 10 show similar results for 80- and 100 μm bubbles, respectively. Although the scattering alternating between reflection and refraction yields a large-phase change in the conventional method, an improvement can be observed if we take both first order refraction and reflection into account. However, more than 20% error can be found when Y > 20 μm. Only very small fluctuation (< 4%) for the phase determination by using the new method can be observed.

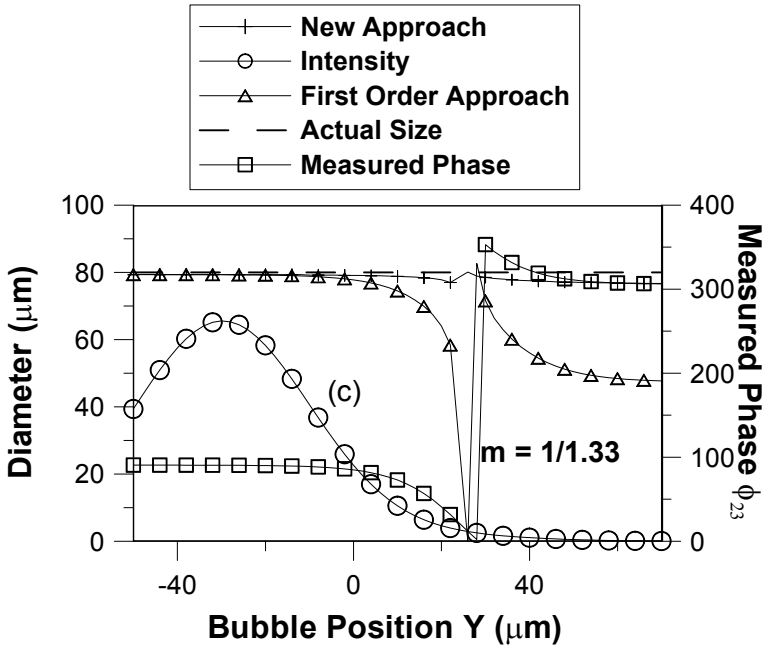

Figure 9 Phase-measurement results among the conventional, the first order and the new approaches

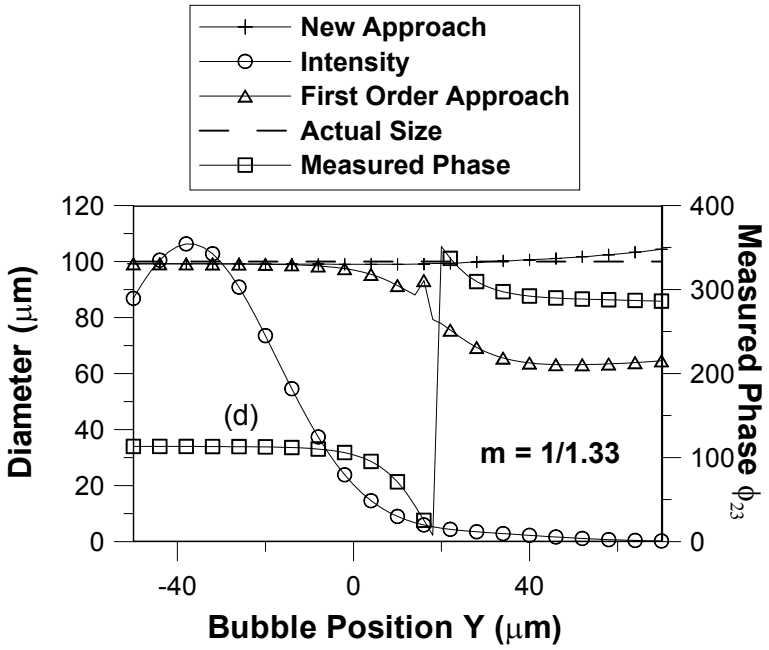

Figure 10 Phase-measurement results among the conventional, the first order and the new approaches

4. Conclusion

A further improvement for PDA measurement free from measurement volume effect was developed in this study for bubble measurements. This new method can effectively eliminate the measurement volume effect including Gaussian beam defect and slit effect by using a four-detectors' PDA system which is very easy to be implemented in two-phase flow measurements. Because no strong validation scheme is necessary other than the signal-to-noise ratio, the measurement volume can be accurately determined by conventional methods, and hence, we have high accuracy in the bubble volume flux and concentration measurements. The performance of this new method was simulated by using GLMT. The newly developed model is especially suitable for sizing particles with refractive index less than one.

5. Acknowledgment

This research was supported by the Hong Kong Government and Hong Kong University of Science and Technology under RGC/EGR (RESEARCH GRANTS COUNCIL/Earmarked Grant for Research) grant No. HKUST 6180/00E.

References

[1] Aizu Y., Durst F., Gréhan G., Onofri F. and Xu T-H. (1993). "PDA systems without Gaussian beam defects.", Presented at *3rd International Conference on Optical Particle Sizing*, Yokohama, Japan, August 23-26.

[2] Saffman M. (1986). "The use of polarized light for optical particle sizing," Presented at *3rd Int. Symposium on Applications of Laser Anemometry to Fluid Mechanics*, Lisbon, Portugal, July 14-17.

[3] Durst F., Tropea C. and Xu T.-H. (1994). "The Slit Effect in Phase Doppler Anemometry*", Proceedings of second International Conference on Fluid Dynamic Measurement and Its Applications*, Edited by X. Shen and X. Sun, Published by International Academic Publishers, Beijing, pp38-43.

[4] Sankar S. V., Inenaga A. S., and Bachalo W. D. (1992). "Trajectory Dependent Scattering in Phase Doppler Interferometer: Minimizing and Eliminating Sizing Errors," *Presented at 6th International Symposium on Applications of Laser Anemometry to Fluid Mechanics*, Lisbon, Portugal, July 20-23.

[5] Grehan G., Gouesbet G., Naqwi A., and Durst F. (1991). "Evaluation of Phase Doppler System using Generalized Lorenz-Mie Theory," Presented at *the International Conference on Multiphase Flows* '91-Tsukuba, Japan, September 24-27, 1991.

[6] Qiu H. -H. and Hsu C. T. (1998). "Optimization of Optical Parameters for Particle Sizing in Multiphase Flows by Using EPDA," *Optics and Laser in Engineering,* Vol. 30, pp3-15.

[7] Qiu H.-H., and Sommerfeld M. (1992). "The impact of signal processing on the accuracy of phase-Doppler measurements," Presented at *the Sixth Workshop on Two Phase Flow Predictions*, Erlangen, Germany, March 30-April 2.

[8] Qiu H. -H. and Hsu C. T. (1996). "A Fourier Optics Method for the Simulation of Measurement-Volume-Effect By the Slit Constraint," Presented at *8th International Symposium on Applications of Laser Techniques to Fluid Mechanics*, Lisbon, Portugal, July 8-11.

[9] Tropea C., Xu T.-H., Onofri F., Gréhan G. and Haugen P. (1994). "Dual Mode Phase Doppler Anemometry," *Presented at 7th International Symposium on Applications of Laser Techniques to Fluid Mechanics*, Lisbon, Portugal, July 8-11.

[10] Qiu H. -H. and Hsu C. T. (1999): "Method of Phase-Doppler Anemometry Free From The Measurement-Volume Effect", *Applied Optics*, Vol 38, Iss 13, pp 2737-2742.

[11] Qiu H.-H , Jia W., Hsu C. T. and Sommerfeld M. (2000): "High Accuracy Optical Particle Sizing in Phase-Doppler Anemometry", *Measurement Science and Technology* , 11,142-151.

[12] Yokoi N., Aizu Y., and Mishina H. (1999): "Estimation of particle trajectory effects and their reduction using polarization in phase Doppler particle measurements," *Optical Engineering*, 38, pp1869-1882.